FEBS Letters 349 (1994) 79–83

FEBS 14257

Solution structure of human interleukin-1 receptor antagonist protein

Brian J. Stockman[a,*], Terrence A. Scahill[a], Nancy A. Strakalaitis[b], David P. Brunner[b], Anthony W. Yem[a], Martin R. Deibel Jr.[a]

[a]*Upjohn Laboratories and* [b]*Chemical Division, The Upjohn Company, 301 Henrietta St., Kalamazoo, MI 49007, USA*

Received 12 May 1994

Abstract

Interleukin-1 receptor antagonist protein (IRAP) is a naturally occurring inhibitor of the interleukin-1 receptor. In contrast to IL-1β, IRAP binds to the IL-1 receptor but does not elicit a physiological response. We have determined the solution structure of IRAP using NMR spectroscopy. While the overall topology of the two 153-residue proteins is quite similar, functionally critical differences exist concerning the residues of the linear amino acid sequence that constitute structurally homologous regions in the two proteins. Structurally homologous residues important for IL-1 receptor binding are conserved between IRAP and IL-1β. By contrast, structurally homologous residues critical for receptor activation are not conserved between the two proteins.

Key words: Interleukin-1β; Interleukin-1 receptor antagonist protein; Protein NMR spectroscopy; Isotopic enrichment

1. Introduction

Interleukin-1β (IL-1β) is a cytokine with inflammatory, immunological and pathological properties (for a review see [1]). The 17 kDa protein binds to two classes of IL-1 receptors, resulting in the mediation of several immune and inflammatory responses and in the induction of a variety of biological changes in neurologic, metabolic, hematologic, and endocrinologic systems [1]. In addition to IL-1β, an interleukin-1 receptor antagonist protein (termed either IRAP or IL-1ra) has been isolated, characterized, cloned and expressed in *E. coli* [2–4]. This newer member of the IL-1 gene family is a naturally occurring inhibitor of the interleukin-1 receptor [2,4], and represents the first described naturally occurring cytokine that functions entirely as a specific receptor antagonist.

Site-directed mutagenesis [5–10] and protein modification [6,11] studies have identified regions of IL-1β that are involved in either receptor binding or transmission of the biological response upon binding. For IRAP, it can be hypothesized that the regions of structure important for receptor binding are maintained, but that the region or regions responsible for eliciting the response are somehow different. To this end, we have determined the solution structure of IRAP using NMR spectroscopy. Since the structure of IL-1β has already been determined by X-ray crystallographic [12–14] and solution NMR spectroscopy [15], a direct comparison between the structures of IRAP and IL-1β can be made. Correlations between structural and biological differences can now be understood at the molecular level.

2. Materials and methods

2.1. Protein

Uniformly ^{15}N- and $^{13}C/^{15}N$-enriched IRAP, a prerequisite for solution structure determination, was prepared using a bacterial expression system as described previously [16]. Samples for NMR spectroscopy typically were 2 mM IRAP, 50 mM $^{2}H_4$-ethanolamine and 300 mM NaCl at pH 6.4. Trace amounts of PMSF and NaN_3 were added to prevent any protease digestion or bacterial growth in the sample. All experiments were recorded at 300 K on a Bruker AMX-600 spectrometer.

2.2. NMR experiments

A variety of NMR experiments were recorded on [^{15}N]IRAP and/or [$^{13}C/^{15}N$]IRAP in order to make sequential resonance assignments, determine the solution secondary structure and provide for the extraction of structural constraints [16–18]. Experimental details and examples of the quality of the IRAP NMR spectra can be found in the references given. In addition to these experiments, two-dimensional ^{1}H-^{15}N HMQC-J [19] and three-dimensional ^{1}H-^{15}N HMQC-NOESY spectra were acquired. The HMQC-J data set was zero-filled four times for a final spectral resolution of 0.5 Hz/pt in the t_1 dimension. $^{3}J_{HN\alpha}$ values, measured from peak splittings, were corrected for the effect of linewidth. The ^{1}H-^{15}N HMQC-NOESY spectrum was acquired without ^{15}N decoupling in o_1, allowing heteronuclear coupling constants to be extracted [20].

2.3. Structural constraints

A total of 683 constraints were used in the calculations. Not including the unassigned ten residues of the N-terminus, this corresponds to 4.8 constraints per residue. A total of 419 NOEs, corresponding to interproton distances, were extracted from two-dimensional ^{1}H-^{1}H NOESY and three-dimensional ^{1}H-^{15}N NOESY-HMQC spectra. The interproton distance constraints were all inter-residue, and were derived from 285 sequential, 21 medium-range (between protons of residues separated by 2–4 residues in the linear sequence) and 113 long-range (between protons of residues > 4 residues apart in the linear sequence) NOEs. Assigned NOEs were classified as strong, medium or weak.

* Corresponding author. Fax: (1) (616) 385-7522.

Abbreviations: DQF-COSY, double quantum filtered correlation spectroscopy; HMQC, heteronuclear multiple quantum correlation; NOE, nuclear Overhauser enhancement; IL-1, interleukin-1; IRAP, interleukin-1 receptor antagonist protein.

SSDI 0014-5793(94)00643-A

Corresponding upper bound constraints were 3.0 Å, 4.0 Å and 5.0 Å. The lower bound constraints used in the calculations were the van der Waals contact radii. Although several hundred intra-residue NOEs were also assigned, they were not incorporated into the structure calculations since they provided little meaningful information. The 419 NOE-derived distance constraints were supplemented with 96 distance constraints assigned to hydrogen bonds based on slowly exchanging amide protons [16]. All 96 distance restraints represented hydrogen bonds between adjacent β-sheet strands.

A total of 168 torsion angle constraints were also incorporated into the calculations, including 68 ϕ values extracted from the ^{1}H-^{15}N HMQC-J spectrum, 70 ψ values derived from ^{13}C chemical shifts [21] and three-bond ^{15}N(i)-^{1}H$^\alpha$(i−1) coupling constants, and 30 χ_1 values. ϕ values were constrained between −160° and −80° for $^3J_{HN\alpha}$ values >8 Hz. ψ values were constrained between 60° and 180° if one of the following conservative criteria was met: $\Delta\delta^{13}C^\alpha$ must be less than −1.0 and $\Delta\delta^{13}C^\beta$ must be greater than 3.0; $\Delta\delta^{13}C^\alpha$ must be less than −1.5 and $\Delta\delta^{13}C^\beta$ must be greater than 2.0; or $\Delta\delta^{13}C^\alpha$ must be less than −2.0 and $\Delta\delta$ $^{13}C^\beta$ must be greater than 1.0. If only one part of a given $\Delta\delta^{13}C$ criteria was met but the three-bond ^{15}N(i)-^{1}H$^\alpha$(i−1) coupling constant was less than 1 Hz, the ψ value was constrained between −20° and −100° (in a non-helical geometry). In two cases, the three-bond ^{15}N(i)-^{1}H$^\alpha$(i−1) coupling constant was 4 Hz, allowing the ψ value to be constrained between −120° and 0°. χ_1 values were defined only when the three-bond ^{15}N(i)-^{1}H$^\beta$(i) coupling constants in the ^{1}H-^{15}N HMQC-NOESY spectrum and the ^{1}H$^\alpha$-^{1}H$^\beta$ correlations in the DQF-COSY spectrum were resolved. χ_1 values were constrained to a ±40° range.

2.4. Structure calculations

All structure calculations were run on a Silicon Graphics Iris Crimson computer using the program DGII from Biosym Technologies Inc. Force constants used were 40 kcal/mol/Å^2 for distance constraints and 40 kcal/mol/rad^2 for torsion angle constraints. An initial energy of 6,000 kcal/mol and a time step of 0.4 ps gave convergence for 13 out of 20 structures calculated using a final DGII error of less than 2.00 as the acceptable criteria. The program Discover from Biosym Technologies Inc. was then used to reduce repulsive non-bonded contacts. Each of the 13 DGII structures was subjected to restrained energy minimization using 100 iterations of steepest descents and 1000 iterations of conjugate gradients. These 13 structures have been deposited in the Brookhaven Protein Data Bank. For the 13 structures, residual NOE and distance restraint violations are small, with no violations greater than 0.5 Å in any structure. The number of violations above 0.3 Å is 1.5 ± 0.7 per structure. Dihedral angle restraint violations were also minimal, with no violations greater than 15° for any structure. For comparison with the NMR solution structure of IL-1β, the average of these 13 structures was calculated and subjected to restrained energy minimization as described above. Since the 10 N-terminal residues have not been assigned and have had no constraints imposed on them, they are not included in any of the figures nor in any of the structural statistics given.

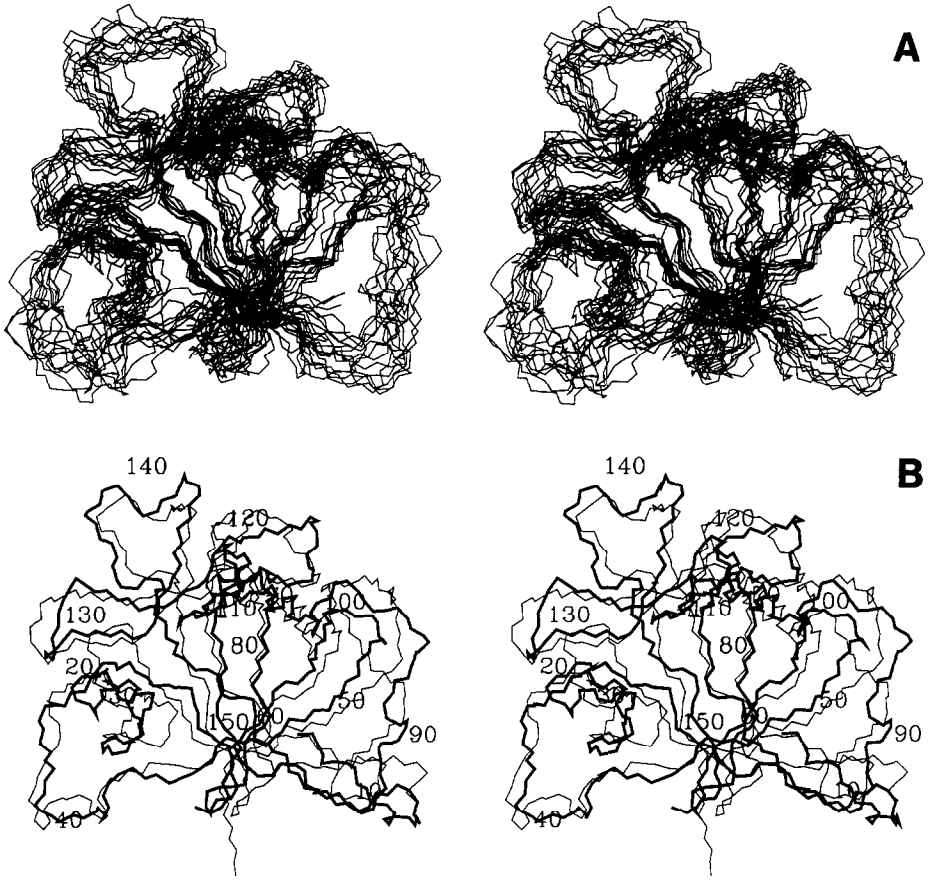

Fig. 1. (A) Stereoview of the superimposed backbone N, C$^\alpha$ and C′ atoms for the 13 calculated structures of IRAP. For alignment, the residue ranges used were 12–27, 30–34, 46–52, 56–84, 100–136 and 147–152. (B) Stereoview of the overlay of the backbone N, C$^\alpha$ and C′ atoms of IRAP (thick line) and IL-1β (thin line). The IRAP structure is numbered every 10 residues. Alignment is based on corresponding β-strands between the two protein: residues 12–27, 30–34, 46–52, 56–84, 100–136 and 147–152 for IRAP and residues 6–21, 25–29, 41–47, 57–85, 100–136 and 146–151 for IL-1β. The IL-1β structure used is that contained in the Brookhaven Protein Data Bank file 6il1b.

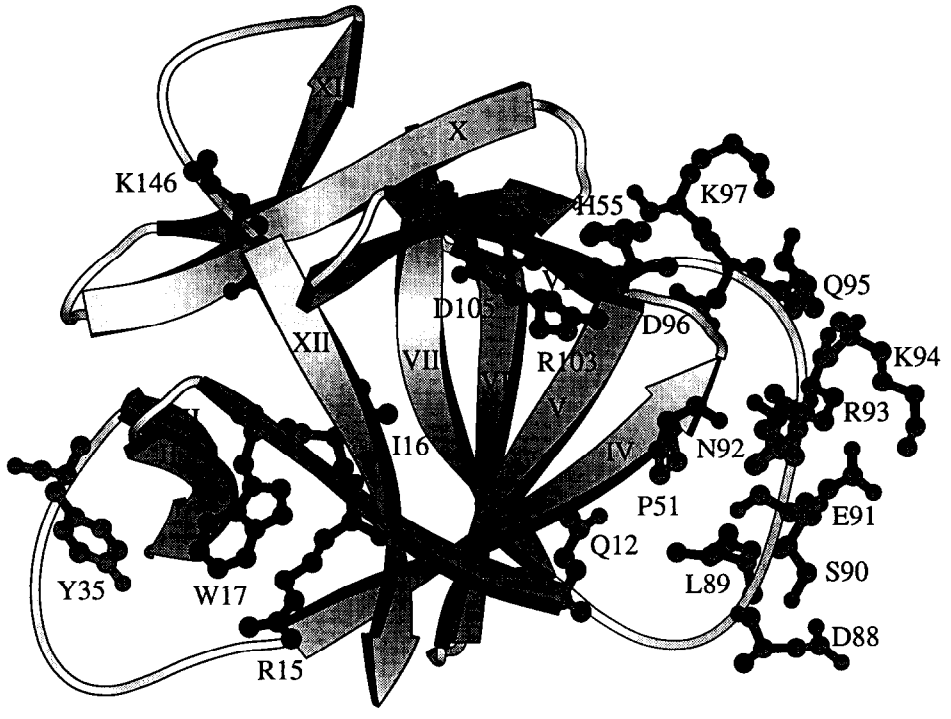

Fig. 2. Ribbon diagram of the average structure of IRAP in the same orientation as in Fig. 1. The β-strands are labeled with Roman numerals. Side chains of residues defined by mutagenesis to be important for receptor binding (grey) and response elicitation (black) are shown. This figure was generated using the program MOLSCRIPT [24].

3. Results and discussion

An overlay of the final 13 IRAP structures is shown in Fig. 1A. The average RMS deviation to the average structure for all heavy atoms is 2.77 ± 0.19 Å and for the backbone N, C^{α} and C′ atoms is 2.03 ± 0.18 Å. The structures shown in Fig. 1A have been superimposed based on the best fit alignment of only residues in the well-defined β-sheet framework of each protein (100 out of the 143 residues). Considering just these residues, the average RMS deviation to the average structure for all heavy atoms is 2.36 ± 0.20 Å and for the backbone N, C^{α} and C′ atoms is 1.67 ± 0.18 Å. As is clear from Fig. 1A, the β-sheet strands are much better defined than the loop regions of IRAP. The topology of the β-sheet strands is more clearly seen in the ribbon diagram of the average IRAP structure shown in Fig. 2. The 12 β-strands are arranged in the same β-trefoil fold topology [22] observed for IL-1β [15,23]. This topology consists of six two-stranded hairpins, three of which form a six-stranded β-barrel (strands XII–I, IV–V and VIII–IX) and three of which cap the barrel (strands II–III, VI–VII and X–XI).

The high level of structural homology between IRAP and IL-1β is apparent from Fig. 1B, which shows an overlay of the backbone atoms of the two proteins. The alignment is based on homologous β-strands as defined previously [16,17]. For this subset of 100 residues, the RMS deviation between the two proteins for the backbone N, C^{α} and C′ atoms is 2.27 Å. While the overall topology of the two 153-residue proteins is quite similar, several functionally critical differences exist concerning the residues of the linear amino acid sequence that constitute structurally homologous regions in the two proteins. The largest differences are at the N-terminus, where the first six residues of IRAP have no structural counterpart in IL-1β, and in the 50's region, where IL-1β has a five-residue insertion beginning at residue 50. Two additional differences, defined on the basis of C^{α} coordinates, are a deletion in IRAP corresponding to residue 24 in IL-1β and a deletion in IL-1β corresponding to residue 142 in IRAP. A third deletion occurs in the 90's region of IL-1β. The exact location cannot be determined because this loop region is poorly defined in the IRAP NMR structure.

The structure of IRAP presented here allows comparisons to be made with the solution structure determined previously for IL-1β [15]. While both proteins bind the IL-1 receptor with the same affinity, only the binding of IL-1β causes activation. A comparison of the two proteins, in the context of site-directed mutagenesis data, provides a basis for understanding the structure–function relationships at the molecular level that underlie the different physiological effects of the two proteins. A summary of residues required for binding or receptor activation as defined by single-site mutants, deletions or loop substitutions [5–10] and chemical modification [6,11] is shown in Fig. 2. The IRAP residues shown

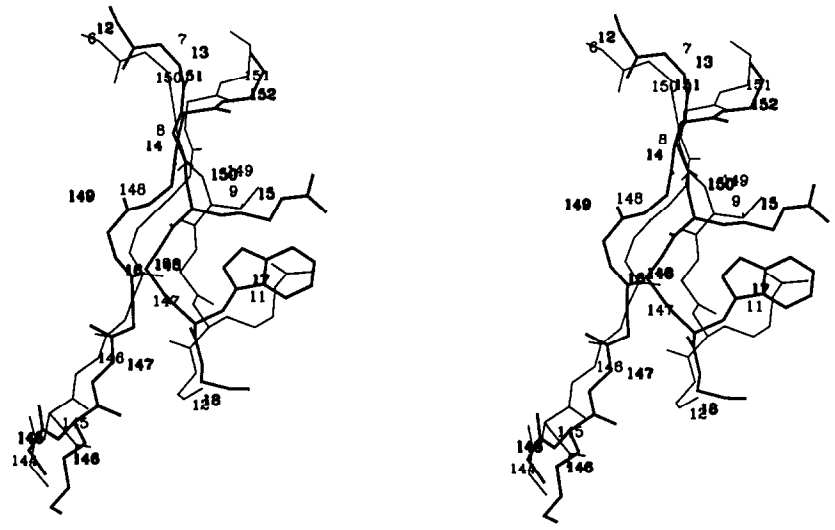

Fig. 3. Stereoview of the overlay of β-strands I and XII of IRAP (thick lines) and IL-1β (thin lines). Alignment is based the backbone N, C^{α} and C′ atoms of residues 12–18 and 145–152 of IRAP with residues 6–12 and 144–151 of IL-1β. Only heavy atoms are shown for the side chains, which differ between the two proteins.

correspond structurally to those residues in IL-1β that have been found to be required for binding or activation.

The majority of the residues important for receptor binding are clustered on one side of the protein encompassing residues 88–105. Residues 12 and 16, located on one side of the N-terminal β-strand, and residue 55 are also involved in receptor binding and are located near the 88–105 region. The hydrophobic or hydrophilic nature of these residues are highly conserved between IRAP and IL-1β providing a rationale for the ability of both proteins to bind to the IL-1 receptor.

Residues T9, R11 and D145 have been defined by site-directed mutagenesis of IL-1β to be critical for receptor activation without effecting receptor binding. The structurally homologous residues in IRAP are R15, W17 and K146. These three residues are located on one face of IRAP as shown in Fig. 2. R15 and W17 are on the same side of the N-terminal β-strand and K146 is located on an adjacent β-strand. An overlay of these two β-strands in IRAP and IL-1β is shown in Fig. 3. The RMS deviation for the backbone N, C^{α} and C′ atoms is 1.15 Å. The orientation of these three side chains with respect to a potential receptor interactions site is very similar between the antagonist and agonist proteins. The lack of conservation between IRAP and IL-1β at these positions, in contrast to what is observed for the structurally homologous receptor-binding residues, is likely to be responsible for the difference in activity between the two proteins.

The structurally homologous IRAP K146 and IL-1β D145 residues shown in Fig. 3 may be especially critical, as they seem to comprise an antagonist/agonist switch. In addition to a D145K mutation in IL-1β, effectively making the agonist IRAP-like at this position, losing the ability to activate the receptor, a K146D mutation in IRAP, effectively making the antagonist IL-1β-like at this position, has been shown to make IRAP into a receptor agonist, albeit a weak one [8].

The solution structure or IRAP presented here complements the previously determined structure of IL-1β. Together they provide a framework to interpret mutagenesis data and suggest potential mutations that might be made to further define the critical regions of the two proteins. The structure suggests that the 88–105 loop of IRAP may be a useful target in the design of small molecules that may mimic IRAP's role as a receptor antagonist. This approach may be limited by the fact that this region is not well defined in the structure (Fig. 1A). This is attributed to a smaller number of assigned NOEs for these residues. In addition, the resonances arising from residues in this region are weak or missing, suggesting conformational heterogeneity. A potential solution may be to determine the conformation as it is bound to the receptor, perhaps by forming a complex between [^{13}C,^{15}N]IRAP and unlabeled receptor. This may lead to the development of small molecules that contain similar functional groups constrained in the same conformation as found in this region of IRAP.

Acknowledgements: We thank Ron VanZanten for assistance with IRAP expression.

References

[1] Dinarello, C.A. (1989) Adv. Immunol. 44, 153–205.
[2] Hannum, C.H., Wilcox, C.J., Arend, W.P., Joslin, F.G., Dripps, D.J., Heimdal, P.L., Armes, L.G., Sommer, A., Eisenberg, S.P. and Thompson, R.C. (1990) Nature 343, 336–340.

[3] Eisenberg, S.P., Evans, R.J., Arend, W.P., Verderber, E., Brewer, M.T., Hannum, C.H. and Thompson, R.C. (1990) Nature 343, 341–346.
[4] Carter, D.B., Deibel, M.R., Jr., Dunn, C.J., Tomich, C.-S.C., Laborde, A.L., Slightom, J.L., Berger, A.E., Bienkowski, M.J., Sun, F.F., McEwan, R.N., Harris, P.K.W., Yem, A.Y., Waszak, G.A., Chosay, J.G., Sieu, L.C., Hardee, M.M., Zurcher-Neely, H.A., Reardon, I.M., Heinrikson, R.L., Truesdell, S.E., Shelly, J.A., Eessalu, T.E., Taylor, B.M. and Tracey, D.E. (1990) Nature 344, 633–638.
[5] MacDonald, H.R., Wingfield, P., Schmeissner, U., Shaw, A., Clore, G.M. and Gronenborn, A.M. (1986) FEBS Lett. 209, 295–298.
[6] Wingfield, P., Graber, P., Shaw, A.R., Gronenborn, A.M., Clore, G.M. and MacDonald, H.R. (1989) Eur. J. Biochem. 179, 565–571.
[7] Gehrke, L., Jobling, S.A., Paik, L.S.K., McDonald, B., Rosenwasser, L.J. and Auron, P.E. (1990) J. Biol. Chem. 265, 5922–5925.
[8] Ju, G., Labriola-Tompkins, E., Campen, C.A., Benjamin, W.R., Karas, J., Plocinski, J., Biondi, D., Kaffka, K.L., Kilian, P.L., Eisenberg, S.P. and Evans, R.J. (1991) Proc. Natl. Acad. Sci. USA 88, 2658–2662.
[9] Labriola-Tompkins, E., Chandran, C., Kaffka, K.L., Biondi, D., Graves, B.J., Hatada, M., Madison, V.S., Karas, J., Kilian, P.L. and Ju, G. (1991) Proc. Natl. Acad. Sci. USA 88, 11182–11186.
[10] Palla, E., Bensi, G., Solito, E., Buonamassa, D.T., Fassina, G., Raugei, G., Spano, F., Galeotti, C., Mora, M., Domenighini, M., Rossini, M., Gallo, E., Carinci, V., Bugnoli, M., Bertini, F., Parente, L. and Melli, M. (1993) J. Biol. Chem. 268, 13486–13492.
[11] Yem, A.W., Guido, D.M., Mathews, W.R., Staite, N.D., Richard, K.A., Prairie, M.D., Krueger, W.C., Epps, D.E. and Deibel, M.R., Jr. (1992) J. Prot. Chem. 11, 709–722.
[12] Finzel, B.C., Clancy, L.L., Holland, D.R., Muchmore, S.W., Watenpaugh, K.D. and Einspahr, H.M. (1989) J. Mol. Biol. 209, 779–791.
[13] Veerapandian, B., Gilliland, G.L., Raag, R., Svensson, A.L., Masui, Y., Hirai, Y. and Poulos, T.L. (1992) Proteins: Str. Funct. Genet. 12, 10–23.
[14] Priestle, J.P., Schar, H.-P. and Grutter, M.G. (1989) Proc. Natl. Acad. Sci. USA 86, 9667–9671.
[15] Clore, G.M., Wingfield, P.T. and Gronenborn, A.M. (1991) Biochemistry 30, 2315–2323.
[16] Stockman, B.J., Scahill, T.A., Roy, M., Ulrich, E.L., Strakalaitis, N.A., Brunner, D.P., Yem, A.W. and Deibel Jr., M.R. (1992) Biochemistry 31, 5237–5245.
[17] Stockman, B.J., Scahill, T.A., Strakalaitis, N.A., Brunner, D.P., Yem, A.W. and Deibel Jr., M.R. (1992) J. Biol. NMR 2, 591–596.
[18] Stockman, B.J., Scahill, T.A., Euvrard, A., Strakalaitis, N.A., Brunner, D.P., Yem, A.W. and Deibel Jr., M.R. (1992) Bull. Magn. Reson 14., 202–207.
[19] Kay, L.E. and Bax, A. (1990) J. Magn. Reson. 86, 110–126.
[20] Montelione, G.T., Winkler, M.E., Rauenbuehler, P. and Wagner, G. (1989) J. Magn. Reson. 82, 198–204.
[21] Spera, S. and Bax, A. (1991) J. Am. Chem. Soc. 113, 5490–5492.
[22] Murzin, A.G., Lesk, A.M. and Chothia, C. (1992) J. Mol. Biol. 223, 531–543.
[23] Driscoll, P.C., Gronenborn, A.M., Wingfield, P.T. and Clore, G.M. (1990) Biochemistry 29, 4668–4682.
[24] Kraulis, P. (1991) J. Appl. Crystallogr. 24, 946–950.